ARTICLE

Variation of Two-Photon Absorption Cross Sections and Optical Limiting of Compounds Induced by Static Electric Field

Yu-jin Zhang, Yu-zhi Song, Chuan-kui Wang*

College of Physics and Electronics, Shandong Normal University, Jinan 250014, China

(Dated: Received on December 1, 2013; Accepted on February 10, 2014)

By numerically solving the Maxwell-Bloch equations using an iterative predictor-corrector finite-difference time-domain technique, we investigate propagating properties of a few-cycle laser pulse in a 4,4′-bis(di-*n*-butylamino) stilbene (BDBAS) molecular medium when a static electric field exists. Dynamical two-photon absorption (TPA) cross sections are obtained and optical limiting (OL) behavior is displayed. The results show that when the static electric field intensity increases, the dynamical TPA cross section is enhanced and the OL behavior is improved. Moreover, both even- and odd-order harmonic spectral components are generated with existence of the static electric field because it breaks the inversion symmetry of the BDBAS molecule. This work provides a method to modulate the nonlinear optical properties of the BDBAS compounds.

Key words: Static electric field, Optical limiting, Two-photon absorption, Organic molecule

I. INTRODUCTION

Taking the mode-locking (Kerr-lens-mode-locking) technique and the chirped pulse amplification technique, one can obtain femtosecond laser pulses with only a few optical cycles in the visible spectrum [1]. Propagation of high intense lasers in a medium gives rise to strong nonlinear effects such as self-phase modulation (SPM), high-order harmonic generation (HHG), two-photon absorption (TPA), and optical limiting (OL). Above all, protecting delicate optical instruments, especially human eye, from intense laser beams motivates a lot of interest in studying OL materials. TPA, a major OL mechanism, was extensively studied during the last decade [2].

Various theoretical methods have been developed to calculate the intrinsic TPA cross sections of organic compounds at *ab initio* level [3−7]. When the TPA cross section of a molecular system is measured, there exists interaction between the molecule and laser. Thus, both simulating experimental results and exploring nonlinear optical processes need to consider the interaction. The previous studies demonstrated that TPA cross sections strongly depend on dynamical parameters of a laser [8−12]. Furthermore, influence of a static electric field on the nonlinear optical properties of compounds has attracted much attention [13−25]. Adorno *et al.* used a Monte Carlo code to describe harmonic generation in presence of an additional static electric field,

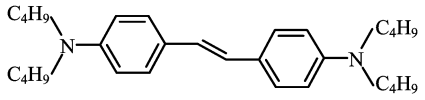

FIG. 1 Molecular structure of 4,4′-bis(di-*n*-butylamino) stilbene (BDBAS).

and the result indicated that even-order harmonics can be generated [16]. Moreover, effects of static electric fields on high harmonic generation were studied by Bao *et al.* [13], and they analyzed the effects by an extension of the zero-range potential model of Becker *et al.* [26]. It was demonstrated that a static electric field changes nonlinear optical properties of media.

The BDBAS molecule has an inversion symmetry (Fig.1), and application of an external static electric field would break the symmetry. As a result, the external static electric field is expected to have obvious influence on the nonlinear optical properties of the BDBAS molecule. In this work, we investigate effects of a static electric field on dynamical TPA cross sections and OL behavior of BDBAS molecular medium for a few-cycle laser pulse. The electronic structures of the BDBAS molecule are calculated at *ab initio* level. Considering the lowest excited states, we model the molecule as a three-level system. The propagation of a few-cycled laser pulse in the molecular medium with the presence of a static electric field is simulated by numerically solving the Maxwell-Bloch equations using an iterative predictor-corrector finite-difference time-domain (FDTD) technique. The OL behavior is displayed and dynamical TPA cross sections are further obtained.

*Author to whom correspondence should be addressed. E-mail: ckwang@sdnu.edu.cn

II. THEORETICAL METHODS AND COMPUTATIONAL DETAILS

The incident electric field is set to be polarized along the x-axis and propagates along the z-axis to an input interface of the medium at z=0, *i.e.*, $\mathbf{E}_l(\mathbf{r},t)$=$E_l(z,t)\hat{\mathbf{x}}$ and $\mathbf{H}(\mathbf{r},t)$=$H_y(z,t)\hat{\mathbf{y}}$. Thus the polarization is $\mathbf{P}$=$P_x\hat{\mathbf{x}}$.

Maxwell equations take the form as

$$\frac{\partial E_l}{\partial z} = -\mu_0 \frac{\partial H_y}{\partial t} \tag{1}$$

$$\frac{\partial H_y}{\partial z} = -\frac{\partial P_x}{\partial t} - \varepsilon_0 \frac{\partial E_l}{\partial t} \tag{2}$$

where μ_0 and ε_0 are the permeability and permittivity of free space, respectively.

The density matrix equations with relaxation effect can be written as follows:

$$\dot{\rho}_{mn} = -\frac{i}{\hbar}[\hat{H},\hat{\rho}]_{mn} - \gamma_{mn}\rho_{mn} \qquad (m \neq n) \tag{3}$$

$$\dot{\rho}_{nn} = -\frac{i}{\hbar}[\hat{H},\hat{\rho}]_{nn} + \sum_{E_m>E_n}\Gamma_{nm}\rho_{mm} - \sum_{E_m<E_n}\Gamma_{mn}\rho_{nn} \tag{4}$$

here, γ_{mn} gives the damping rate of ρ_{mn}, and Γ_{nm} gives the rate per molecule at which population decays from level m to level n. $\hat{H}$ is the Hamiltonian of the system, which includes the free Hamiltonian of the molecule $\hat{H}_0$ and the interaction Hamiltonian $\hat{H}'$. Within the dipole approximation, the interaction Hamiltonian can be expressed as

$$\hat{H}' = -\hat{\boldsymbol{\mu}} \cdot (\mathbf{E}_l + \mathbf{E}_s) \tag{5}$$

where $\hat{\boldsymbol{\mu}}$ is the electric dipole moment operator, $\mathbf{E}_l$ and $\mathbf{E}_s$ are the incident electric field and the static electric field.

The macroscopic nonlinear polarization P_x is related to ensemble average of the expectation value of the dipole moment operator for a molecule,

$$P_x = N\langle\hat{\mu}_x\rangle = N\mathrm{tr}(\hat{\mu}_x\hat{\rho}) \tag{6}$$

where N is molecular density and set to be N=7×10^{25} m^{-3} in this work [27].

Considering an one-dimensional structure of the molecule (assumed in the x direction) and only three states are included, one can thus simplify the Bloch equations with the definition of

$$\rho_{01} = \frac{u_0 + i\nu_0}{2} \tag{7}$$

$$\rho_{12} = \frac{u_1 + i\nu_1}{2} \tag{8}$$

$$\rho_{02} = \frac{u_2 + i\nu_2}{2} \tag{9}$$

$$\frac{\partial u_0}{\partial t} = -\omega_{10}\nu_0 + \frac{(\mathbf{E}_l+\mathbf{E}_s)\cdot(\boldsymbol{\mu}_{11}-\boldsymbol{\mu}_{00})}{\hbar}\nu_0 + \frac{(\mathbf{E}_l+\mathbf{E}_s)\cdot(\boldsymbol{\mu}_{12}\nu_2+\boldsymbol{\mu}_{02}\nu_1)}{\hbar} - \gamma_{01}u_0 \tag{10}$$

$$\frac{\partial \nu_0}{\partial t} = \omega_{10}u_0 - \frac{(\mathbf{E}_l+\mathbf{E}_s)\cdot(\boldsymbol{\mu}_{12}u_2-\boldsymbol{\mu}_{02}u_1)}{\hbar} - \frac{(\mathbf{E}_l+\mathbf{E}_s)\cdot(\boldsymbol{\mu}_{11}-\boldsymbol{\mu}_{00})}{\hbar}u_0 - \frac{2}{\hbar}(\mathbf{E}_l+\mathbf{E}_s)\cdot\boldsymbol{\mu}_{01}(\rho_{00}-\rho_{11}) - \gamma_{01}\nu_0 \tag{11}$$

$$\frac{\partial u_1}{\partial t} = -\omega_{21}\nu_1 + \frac{(\mathbf{E}_l+\mathbf{E}_s)\cdot(\boldsymbol{\mu}_{22}-\boldsymbol{\mu}_{11})}{\hbar}\nu_1 - \frac{(\mathbf{E}_l+\mathbf{E}_s)\cdot(\boldsymbol{\mu}_{02}\nu_0+\boldsymbol{\mu}_{01}\nu_2)}{\hbar} - \gamma_{12}u_1 \tag{12}$$

$$\frac{\partial \nu_1}{\partial t} = \omega_{21}u_1 - \frac{(\mathbf{E}_l+\mathbf{E}_s)\cdot(\boldsymbol{\mu}_{22}-\boldsymbol{\mu}_{11})}{\hbar}u_1 - \frac{(\mathbf{E}_l+\mathbf{E}_s)\cdot(\boldsymbol{\mu}_{02}u_0+\boldsymbol{\mu}_{01}u_2)}{\hbar} - \frac{2}{\hbar}(\mathbf{E}_l+\mathbf{E}_s)\cdot\boldsymbol{\mu}_{12}(\rho_{11}-\rho_{22}) - \gamma_{12}\nu_1 \tag{13}$$

$$\frac{\partial u_2}{\partial t} = -\omega_{20}\nu_2 + \frac{(\mathbf{E}_l+\mathbf{E}_s)\cdot(\boldsymbol{\mu}_{22}-\boldsymbol{\mu}_{00})}{\hbar}\nu_2 + \frac{(\mathbf{E}_l+\mathbf{E}_s)\cdot(\boldsymbol{\mu}_{12}\nu_0+\boldsymbol{\mu}_{01}\nu_1)}{\hbar} - \gamma_{02}u_2 \tag{14}$$

$$\frac{\partial \nu_2}{\partial t} = \omega_{20}u_2 - \frac{(\mathbf{E}_l+\mathbf{E}_s)\cdot(\boldsymbol{\mu}_{22}-\boldsymbol{\mu}_{00})}{\hbar}u_2 - \frac{(\mathbf{E}_l+\mathbf{E}_s)\cdot(\boldsymbol{\mu}_{12}u_0-\boldsymbol{\mu}_{01}u_1)}{\hbar} - \frac{2}{\hbar}(\mathbf{E}_l+\mathbf{E}_s)\cdot\boldsymbol{\mu}_{02}(\rho_{00}-\rho_{22}) - \gamma_{02}\nu_2 \tag{15}$$

$$\frac{\partial \rho_{00}}{\partial t} = \frac{(\mathbf{E}_l+\mathbf{E}_s)\cdot(\boldsymbol{\mu}_{01}\nu_0+\boldsymbol{\mu}_{02}\nu_2)}{\hbar} + \Gamma_{01}\rho_{11} + \Gamma_{02}\rho_{22} \tag{16}$$

$$\frac{\partial \rho_{11}}{\partial t} = -\frac{(\mathbf{E}_l+\mathbf{E}_s)\cdot(\boldsymbol{\mu}_{01}\nu_0-\boldsymbol{\mu}_{12}\nu_1)}{\hbar} + \Gamma_{12}\rho_{22} - \Gamma_{01}\rho_{11} \tag{17}$$

$$\frac{\partial \rho_{22}}{\partial t} = -\frac{(\mathbf{E}_l+\mathbf{E}_s)\cdot(\boldsymbol{\mu}_{02}\nu_2+\boldsymbol{\mu}_{12}\nu_1)}{\hbar} - \Gamma_{02}\rho_{22} - \Gamma_{12}\rho_{22} \tag{18}$$

here, $\boldsymbol{\mu}_{mn}$ is the transition electric dipole moment between level m and n, $\boldsymbol{\mu}_{nn}$ is the permanent electric dipole moment of level n, and $\hbar\omega_{mn}$ is the excitation energy between the states m and n.

In the absence of significant recombination, diffusion and thermal runaway, the differential equation of the field intensity in the presence of one-photon absorption and TPA can be written as [28]

$$\frac{\mathrm{d}I}{\mathrm{d}z} + \alpha I + \beta I^2 = 0 \tag{19}$$

where I is the field intensity, α denotes the linear absorption coefficient, and β is the TPA coefficient. The analytical solution of Eq.(19) is

$$I(z) = \frac{\alpha I(0)\exp(-\alpha z)}{\alpha + \beta I(0)[1-\exp(-\alpha z)]} \tag{20}$$

DOI:10.1063/1674-0068/27/03/259-264

TABLE I The excitation energies E_n, oscillator strengths $\delta_{\rm op}$ and dipole moments μ_{mn} of the first five excited states n.

n	E_n/eV	$\delta_{\rm op}$/Arb. unit	μ_{0n}/a.u.	μ_{1n}/a.u.	μ_{2n}/a.u.	μ_{3n}/a.u.	μ_{4n}/a.u.	μ_{5n}/a.u.
1	3.4081	1.6303	4.3970	0.0232				
2	4.0656	0.0006	0.0554	0.8054	0.0135			
3	4.0729	0.1486	1.0699	0.0654	0.1817	0.0154		
4	4.2058	0.0002	0.0380	4.8984	0.0290	0.4397	0.0260	
5	4.9443	0.0026	0.0696	0.1658	3.0484	3.9450	0.5531	0.0260

If $I(0)$ is smaller than the saturation absorption intensity, the TPA coefficient β can be assumed as a linear function of $I(0)$,

$$\beta = \beta_0 - cI(0) \tag{21}$$

where β_0 is the steady-state TPA coefficient and c is a constant [28]. Eq.(20) can be reformed as

$$\begin{aligned}\frac{1}{T} &= \frac{I(0)}{I(z)} \\ &= \exp(\alpha z) + \frac{[\exp(\alpha z)-1]\beta_0}{\alpha} I(0) - \\ &\quad \frac{c[\exp(\alpha z)-1]}{\alpha} I^2(0)\end{aligned} \tag{22}$$

where T is the intensity transmission at the propagation distance z. The values of α and β_0 can thus be determined by fitting the input-output pulses' peak intensity through Eq.(22). The molecular TPA cross section σ_{tp} is related to β_0 by

$$h\nu\beta_0 = \sigma_{\rm tp} N \tag{23}$$

where $h\nu$ is the input photon energy.

The Maxwell equations and Bloch equations are coupled with each other through the macroscopic dipole moment P_x expressed in Eq.(6). In simulations, we solve numerically the Maxwell-Bloch equations with the predictor-corrector FDTD methods [29, 30]. Time-dependent DFT/B3LYP method implemented in DALTON package [31] is employed to calculate the lowest five excited states of the molecule as shown in Table I, in which the 6-31G basis set is used. One can see that the molecule can be well described by a three-level model (Fig.2) in low energy region, where S_0, S_1, and S_2 are the ground, first excited, and fourth excited states respectively, when the interaction between laser and the molecule is dealt with. The transition dipole moments among the states are μ_{01x}=4.3970 a.u., μ_{12x}=4.8984 a.u., respectively, while the components along y-axis and z-axis are approximately equal to zero due to the one-dimension property of the molecule. The transition between S_0 and S_2 is dipole forbidden. The permanent dipole moments of these states are also equal to zero because of the inversion symmetry of the molecule. The excitation energies of the S_1 and S_2 states are $\hbar\omega_{10}$=3.4081 eV and $\hbar\omega_{20}$=4.2058 eV, respectively. The molecule is assumed to be at its ground state S_0 before the excitation laser pulse is switched on, namely, $\rho_{00}(t{=}0){=}1$, $\rho_{11}(t{=}0){=}\rho_{22}(t{=}0){=}0$. The decay rates of the density matrix elements γ_{nm} can be chosen as 10^{13} s^{-1}, while the decay rates of excited states Γ_{01}, Γ_{12} and Γ_{02} are assumed to be equal to 10^9, 10^{12}, and 0 s^{-1}, respectively [32, 33].

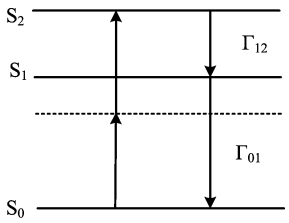

FIG. 2 Scheme of three energy levels.

The incident excitation pulse is modeled with a hyperbolic-secant shape as follows,

$$\begin{aligned}E_l(t=0,z) = F_0 \mathrm{sech}\left(1.76\frac{z/c+z_0/c}{\tau}\right) \cdot \\ \cos\left(\omega_p \frac{z+z_0}{c}\right)\end{aligned} \tag{24}$$

where F_0 is the peak amplitude of the pulse, τ is the full width at half maximum (FWHM) of the intensity profile of the pulse. The choice of z_0 ensures that the pulse penetrates negligibly into the medium at t=0. The carrier wave frequency of the incident field is taken to be half of the frequency between the S_0 and S_2 states ($\omega_p{=}\omega_{20}/2$), *i.e.*, the two-photon resonant frequency of the fourth excited state. In the following numerical simulations, the FWHM of the incident excitation pulse is set to be 5 fs unless otherwise noted. The static electric field E_s is put along the x-direction which has the same direction as the few-cycle laser field.

III. RESULTS AND DISCUSSION

A. Propagation of the ultrashort pulse

We firstly investigate propagation of the ultrashort pulse when the static electric field is absent. The tem-

DOI:10.1063/1674-0068/27/03/259-264

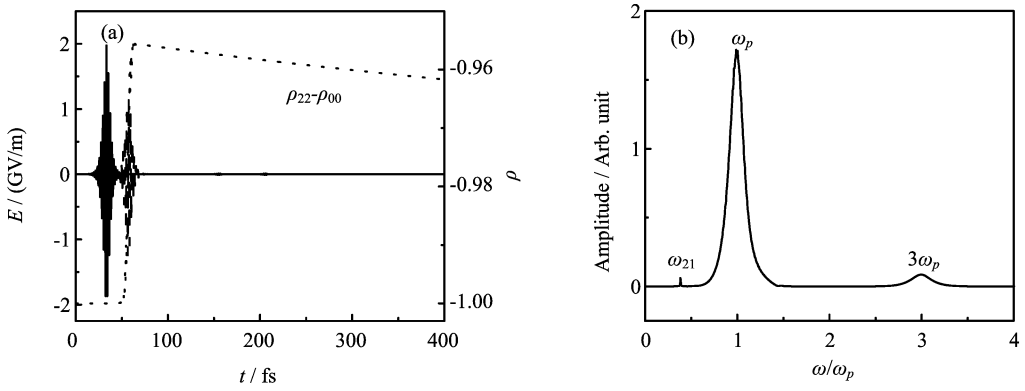

FIG. 3 Pulse propagation through the BDBAS medium without a static electric field. (a) Carrier wave of the pulse at propagation distance of 0 μm (solid line) and 7.0 μm (dashed line), and population difference $\rho_{22}-\rho_{00}$ (dotted line) at the propagation distance of 7.0 μm. (b) The corresponding spectrum at 7.0 μm. F_0=2.0×10^9 V/m, τ=5 fs.

poral evolution of the field at the propagation distances of 0 and 7.0 μm in the medium and the population difference at 7.0 μm are shown in Fig.3(a). We can see that the pulse propagates without split and the population difference between the states S_0 and S_2 changes slightly. The correspondent spectrum is displayed in Fig.3(b). Appearance of a frequency component ω_{21} is caused by existence of radiation from the states S_2 to S_1. Besides, an odd harmonic component $3\omega_p$ appears due to the four-wave mixing effect, while even harmonic components are restrained because of the inversion symmetry of the molecule.

When a static electric field is applied, propagation of the few-cycle laser pulse and the corresponding spectra are shown in Fig.4. It can be found that the static electric field has a large effect on the pulse propagation. Firstly, the pulse is obviously split and sub-pulses appear. Secondly, the population difference, $\rho_{22}-\rho_{00}$, is enhanced compared to the case in Fig.3. Thirdly, it is very interesting to note that even-order spectral components $2\omega_p$ and $4\omega_p$ are produced during the pulse propagation. It indicates that the transition between S_2 and S_0 is permitted by applying the static electric field. In our theoretical model, when a static field $\mathbf{E}_s$ exists, the total Hamiltonian operator is expressed as follows,

$$\begin{aligned}\hat{H} &= \hat{H}_0 - \hat{\boldsymbol{\mu}}(\mathbf{E}_l + \mathbf{E}_s) \\ &= \hat{H}_0^N - \hat{\boldsymbol{\mu}}\mathbf{E}_l \qquad (25)\\ \hat{H}_0^N &= \hat{H}_0 - \hat{\boldsymbol{\mu}}\mathbf{E}_s \qquad (26)\end{aligned}$$

where $\hat{H}_0^N$ represents the Hamiltonian operator of the molecule influenced by the static field. Thus, taking the eigenfunctions $\{\psi_n\}$ of $\hat{H}_0$ as the basis set, we formulate the matrix formulation of $\hat{H}_0^N$ for our simplified system as

$$\hat{H}_0^N = \begin{pmatrix} E_1-\mu_{11}E_s & -\mu_{12}E_s & -\mu_{13}E_s \\ -\mu_{21}E_s & E_2-\mu_{22}E_s & -\mu_{23}E_s \\ -\mu_{31}E_s & -\mu_{32}E_s & E_3-\mu_{33}E_s \end{pmatrix} \qquad (27)$$

The eigenfunctions $\{\Phi_1,\Phi_2,\Phi_3\}$ of $\hat{H}_0^N$ are a linear combination of the eigenfunctions $\{\psi_1,\psi_2,\psi_3\}$. It is observed that these eigenfunctions $\{\Phi_1,\Phi_2,\Phi_3\}$ have no certain parity on the basis of the inversion symmetry of the molecule, which can be described as the breakdown of the inversion symmetry caused by the static field. As a result, when a static field $\mathbf{E}_s$ exists, our theoretical methods demonstrate that even-order spectral components appear as the laser pulse propagates in the molecular medium.

Furthermore, one can see that the frequency broadening of the second harmonic peak is much narrower than that of the third harmonic peak, indicating better temporal coherence for the second harmonic. The reason is that the second harmonic generation comes from the transition from the state S_2 to S_0, where the lifetime of S_2 is about 1 ps in our simulation as shown above. Thus, the frequency broadening for the second harmonic peak is about $\Delta\omega\approx10^{-4}\omega_p$, which is much narrower than that of the third harmonic peak that comes from four-wave mixing including the input laser pulse with a frequency broadening of $\Delta\omega\approx0.19\omega_p$.

In addition, there are obvious oscillatory features appearing around the even- and odd-order frequency, which is supposed to be a result of the interference of separated pulses with the corresponding spectral components [34]. As the static field intensity increases, comparing Fig.4 (a) and (b) with (c) and (d), one can see that the tail of the main-pulse caused by the spontaneous radiation becomes more obvious, the population difference turns larger, and amplitudes of the even-order spectral components are stronger.

B. OL and dynamical TPA cross section of BDBAS

To illustrate the influence of static electric fields on OL property of the molecular medium, we present the output peak intensity $I_{\rm out}$ as a function of the input peak intensity $I_{\rm in}$ at the propagation distance of 7.0 μm

DOI:10.1063/1674-0068/27/03/259-264

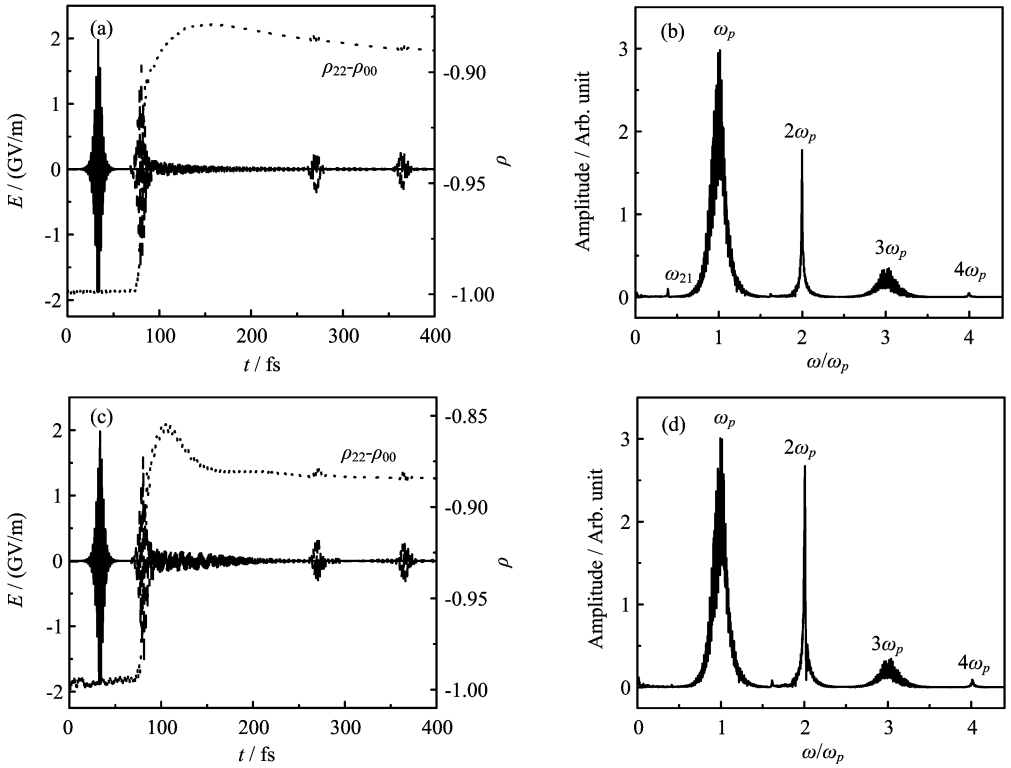

FIG. 4 Pulse propagation through the BDBAS medium with a static electric field. Carrier wave of the pulse at propagation distances of 0 μm (solid line) and 7.0 μm (dashed line), and population difference $\rho_{22}-\rho_{00}$ (dotted line) at a propagation distance of 7.0 μm (a) with E_s=0.15F_0 and (c) with E_s=0.3F_0. The corresponding spectra (b) and (d) at 7.0 μm. F_0=2.0 GV/m, τ=5 fs.

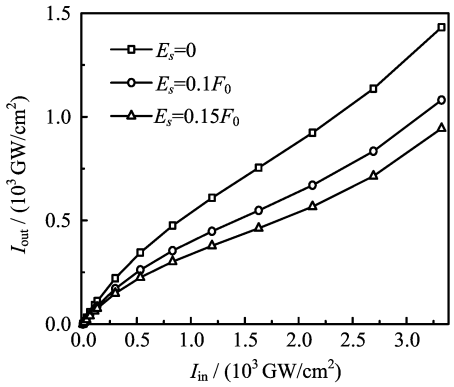

FIG. 5 Output peak intensity $I_{\rm out}$ versus the input peak intensity $I_{\rm in}$ at the propagation distance of 7.0 μm with different static fields E_s=0, 0.1F_0, and 0.15F_0. τ=5 fs.

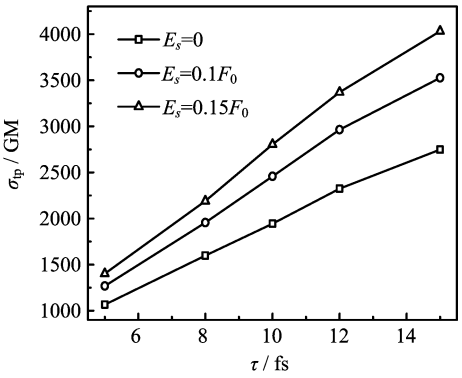

FIG. 6 Dependence of TPA cross section $\sigma_{\rm tp}$ on the static field intensity E_s and the pulse width τ at the propagation distance of 7.0 μm.

with different amplitudes of static electric fields, E_s=0, 0.1F_0, 0.15F_0, in Fig.5. One can clearly see that with small input intensity $I_{\rm in}\leq$100 GW/cm^2, the curves are nearly linear and the same for the three cases, which indicates weak nonlinear absorption of the medium due to the TPA process. When the input intensity is larger than 100 GW/cm^2, it is evident that the output intensity $I_{\rm out}$ in the case with a static electric field is smaller than that without a static electric field, showing more obvious OL behavior with the consideration of a static electric field. Furthermore, as the intensity of the static electric field increases, the intensity of the output intensity decreases.

Using the input-output peak-intensity relation in the OL region obtained above, we calculate the dynamical TPA cross section of the organic molecule. Dependence of TPA cross sections on the static electric field and the pulse width is shown in Fig.6. When the intensity of

DOI:10.1063/1674-0068/27/03/259-264

the static electric field increases, the dynamical values of the TPA cross sections are enhanced. For example, the TPA cross sections for 10 fs pulse are 1943, 2457, and 2803 GM (1 GM=10^{-50} cm^4s/photon) for E_s=0, $0.1F_0$, and $0.15F_0$, respectively, while the intrinsic TPA cross section of the molecule is σ_{tp}=1430 GM on the basis of the *ab initio* calculation. The enhancement of the TPA cross section with the static electric field mainly attributes to the appearance of the spectral component $2\omega_p$ with a relative large amplitude, which gives an additional contribution for the resonant transition from the state S_0 to S_2.

Moreover, one can see that σ_{tp} increases with the increase of τ almost linearly. The main mechanism is that the TPA process keeps longer for larger pulse widths that makes a larger contribution to the absorption from S_0 to S_2.

IV. CONCLUSION

In this work, we have theoretically studied the effect of static electric fields on the propagation and spectrum as well as OL behavior and dynamical TPA cross sections of a few-cycle ultrashort laser pulse in BDBAS by solving the Maxwell-Bloch equations. It is found that, when a static electric field is present, split of the pulse is enhanced and even-order spectral components can be generated. Moreover, OL behavior becomes obvious with the assistance of a static electric field. Dynamical TPA cross sections increase with higher static field intensities and wider laser pulse widths. Our results suggest an approach to enhance the nonlinear optical properties of the compounds by applying a static electric field.

V. ACKNOWLEDGMENTS

This work was supported by the 973 Program (No.2011CB808100). Partial computation is carried on the high performance computing supported by China Educational Television and guoshi.com.

[1] T. Brabec and F. Krausz, Rev. Mod. Phys **72**, 545 (2000).
[2] P. N. Prasad, *Introduction to Biophotonics*, New Jersey: Kluwer Academic Publishers, 593 (2003).
[3] P. Macak, Y. Luo, P. Norman, and H. Ågren, J. Chem. Phys. **113**, 7055 (2000).
[4] C. K. Wang, P. Macak, Y. Luo, and H. Ågren, J. Chem. Phys. **114**, 9813 (2001).
[5] P. Sałek, O. Vahtras, T. Helgaker, and H. Ågren, J. Chem. Phys. **117**, 9630 (2002).
[6] P. Cronstrand, Y. Luo, and H. Ågren, J. Chem. Phys. **117**, 11102 (2002).
[7] H. J. Ding, J. Sun, and C. K. Wang, Chin. J. Chem. Phys. **25**, 666 (2012).
[8] A. Baev, F. Gel'mukhanov, P. Macák, Y. Luo, and H. Ågren, J. Chem. Phys. **117**, 6214 (2002).
[9] J. C. Liu, V. C. Felicíssimo, F. F. Guimarães, C. K. Wang, and F. Gel'mukhanov, J. Phys. B **41**, 074016 (2008).
[10] J. C. Liu, C. K. Wang, and F. Gel'mukhanov, Phys. Rev. A **76**, 053804 (2007).
[11] C. K. Wang, J. C. Liu, K. Zhao, Y. P. Sun, and Y. Luo, J. Opt. Soc. Am. B **24**, 2436 (2007).
[12] C. K. Wang, P. Zhao, Q. Miao, Y. P. Sun, and Y. Zhou, J. Phys. B **43**, 105601 (2010).
[13] M. Q. Bao and A. F. Starace, Phys. Rev. A **53**, R3723 (1996).
[14] B. Borca, A. V. Flegel, M. V. Frolov, N. L. Manakov, D. B. Milošević, and A. F. Starace, Phys. Rev. Lett. **85**, 732 (2000).
[15] T. Zuo, A. D. Bandrauk, M. Ivanov, and P. B. Corkum, Phys. Rev. A **51**, 3991 (1995).
[16] D. P. Adorno, G. Ferrante, and M. Zarcone, J. Comput. Electron. **6**, 31 (2007).
[17] B. Wang, X. Li, and P. Fu, Phys. Rev. A **59**, 2894 (1999).
[18] B. Wang, X. Li, and P. Fu, J. Phys. B **31**, 1961 (1998).
[19] S. Odžak and D. B. Milošević, Phys. Rev. A **72**, 033407 (2005).
[20] D. B. Milošević and A. F. Starace, Phys. Rev. Lett. **81**, 5097 (1998).
[21] D. B. Milošević and A. F. Starace, Phys. Rev. A **60**, 3943 (1999).
[22] F. Filsinger, J. Küpper, G. Meijer, L. Holmegaard, J. H. Nielsen, I. Nevo, J. L. Hansen, and H. Stapelfeldt, J. Chem. Phys. **131**, 064309 (2009).
[23] Y. Xiang, Y. P. Niu, and S. Q. Gong, Phys. Rev. A **79**, 053419 (2009).
[24] C. L. Xia, G. T. Zhang, J. Wu, and X. S. Liu, Phys. Rev. A **81**, 043420 (2010).
[25] C. S. Praveen, A. Kokalj, M. Rérat, and M. Valant, Solid State Sci. **14**, 1412 (2012).
[26] W. Becker, S. Long, and J. K. McIver, Phys. Rev. A **50**, 1540 (1994).
[27] J. E. Ehrlich, X. L. Wu, I. Y. S. Lee, Z. Y. Hu, H. Röckel, S. R. Marder, and J. W. Perry, Opt. Lett. **22**, 1843 (1997).
[28] J. D. Bhawalkar, G. S. He, and P. N. Prasad, Rep. Prog. Phys. **59**, 1041 (1996).
[29] R. W. Ziolkowski, J. M. Arnold, and D. M. Gogny, Phys. Rev. A **52**, 3082 (1995).
[30] A. V. Tarasishin, S. A. Magnitskii, V. A. Shuvaev, and A. M. Zheltikov, Opt. Express **8**, 452 (2001).
[31] DALTON.A Molecular Electronic Structure Program, Release Dalton 2011 (2011), http://dalton-program.org/.
[32] F. Gel'mukhanov, A. Baev, P. Mack, Y. Luo, and H. Ågren, J. Opt. Soc. Am. B **19**, 937 (2002).
[33] S. Gavrilyuk, S. Polyutov, P. C. Jha, Z. Rinkevicius, H. Ågren, and F. Gel'mukhanov, J. Phys. Chem. A **111**, 11961 (2007).
[34] K. Zhao, J. C. Liu, C. K. Wang, and Y. Luo, Chin. Phys. **14**, 2014 (2005).

DOI:10.1063/1674-0068/27/03/259-264